ANL/ET/CP-102885

SMOOTH- AND ENHANCED-TUBE HEAT TRANSFER AND PRESSURE DROP: PART I. EFFECT OF PRANDTL NUMBER WITH AIR, WATER, AND GLYCOL/WATER MIXTURES*

N. T. Obot,[1] L. Das,[2] and T. J. Rabas[3]

[1]Argonne National Laboratory, Argonne, Illinois 60439, USA; E-mail: obot@anl.gov;

Professor Emeritus, Department of Chemical Engineering, Clarkson University, Potsdam, NY 13699, USA

[2]Former Graduate Student, Department of Chemical Engineering, Clarkson University, Potsdam, NY, USA

[3]Argonne National Laboratory, Argonne, Illinois 60439, USA

October 2000

To be presented at Third International Conference on Compact Heat Exchangers and Enhancement Technology for the Process Industries, Davos, Switzerland, July 1-6, 2001.

*Work partially supported by the U.S. Department of Energy, Energy Efficiency and Renewable Energy, under Contract W-31-109-Eng-38.

DISCLAIMER

DISCLAIMER

Portions of this document may be illegible in electronic image products. Images are produced from the best available original document.

SMOOTH- AND ENHANCED-TUBE HEAT TRANSFER AND PRESSURE DROP: PART I. EFFECT OF PRANDTL NUMBER WITH AIR, WATER, AND GLYCOL/WATER MIXTURES

N. T. Obot,[1] L. Das,[2] and T. J. Rabas[3]

[1]Argonne National Laboratory, Argonne, Illinois 60439, USA; E-mail: obot@anl.gov;
Professor Emeritus, Department of Chemical Engineering, Clarkson University, Potsdam, NY 13699, USA
[2]Former Graduate Student, Department of Chemical Engineering, Clarkson University, Potsdam, NY, USA
[3]Argonne National Laboratory, Argonne, Illinois 60439, USA

ABSTRACT

An extensive experimental investigation was carried out to determine the pressure drop and heat transfer characteristics in laminar, transitional, and turbulent flow through one smooth tube and twenty-three enhanced tubes. The working fluids for the experiments were air, water, ethylene glycol, and ethylene glycol/water mixtures; Prandtl numbers (*Pr*) ranged from 0.7 to 125.3. The smooth-tube experiments were carried out with *Pr* values of 0.7, 6.8, 24.8, 39.1, and 125.3; *Pr* values of 0.7, 6.8, and 24.8 were tested with enhanced tubes. Reynolds number (*Re*) range (based on the maximum internal diameter of a tube) was 200 to 55,000, depending on Prandtl number and tube geometry. The results are presented and discussed in this paper.

INTRODUCTION

Extensive experimental studies on the pressure-drop and heat-transfer characteristics of a wide range of enhanced surface geometries have been published by numerous researchers. The results of these studies indicate that varying amounts of pressure-drop and heat-transfer increases can be realized with enhanced tubes, depending on the geometric characteristics of the surfaces. Reviews of the widespread literature were presented by several researchers (Reay, 1991; Obot *et al.* 1990; Rabas, 1989; Webb, 1987; Ravigururajan and Bergles, 1986).

A search of the literature reveals very limited studies with commercially available enhanced tubes over the entire range of flow conditions extending from laminar through turbulent flow. With the exception of the studies by Obot *et al.* (1994), Esen *et al.* (1994), Esen (1992) and Das (1993), virtually all the investigations with tubes of the spirally fluted type were confined to either turbulent flow (Yampolsky *et al.*, 1984; Panchal and France, 1986; Ravigururajan and Bergles, 1986) or laminar and transitional flow (Shome and Jensen, 1996). Similarly, for corrugated surfaces of single and multiple helix (Withers, 1980a,b) or three-dimensional spiral ribs (Takahashi et *al.*, 1985), pressure drop and heat transfer data were reported only for turbulent flow.

In sharp contrast to turbulent flow, limited experimental data on pressure drop and heat transfer in laminar flow and the transition region exist for enhanced passages (Shome and Jensen, 1996; Marner and Bergles, 1978; Watkinson *et al.*, 1974; Koch, 1960; Nunner, 1956). In the recent study by Shome and Jensen with internally-finned tubes, the Reynolds and Prandtl number ranges were 150 to 2,000 and 50 to 185, respectively.

Another problem that has not received much attention is the effect of fluid properties on enhanced-tube heat transfer that is usually expressed in nondimensional form by using the Prandtl number (*Pr*). *A* search of the literature revealed only a handful of studies with more than one fluid (Webb *et al.*, 1971; Marner and Bergles, 1978; Carnavos, 1980; Smith and Gowen, 1985; Gomelauri, 1964). Alternatively, in some previous studies with liquids, the Prandtl number was varied by adjusting the bulk temperature of the fluid (Shome and Jensen, 1996; Dipprey and Sabersky, 1963; Watkinson *et al.*, 1974). The drawback with this approach is that the observed heat-transfer trends with increasing *Pr* may not form the basis for generally valid conclusions because of the restricted range. There is a need for a comprehensive investigation of the effect of Prandtl number on pressure-drop and heat-transfer performance of enhanced tubes.

Although the problem has been studied extensively, high-quality heat-transfer and pressure-drop prediction methods for enhanced tubes are very limited and/or nonexistent. The reason is that too many variables are involved and it is difficult to develop a predictive method that accurately accounts for the effects of these variables. A recent effort focused on the *frictional law of corresponding states*, the basis of which is the transition from laminar to turbulent flow (Obot *et al.*, 1994). There is a need to validate the frictional law analysis for a range of *Pr* values.

In summary, pressure-drop and heat-transfer data are needed for a wide range of enhancement geometries to fill

the gaps in the existing literature data base; notably, laminar and transitional flow data are needed because these regions have received very meager treatment in the past. Also, the general state of knowledge on the effect of Prandtl number on pressure drop and heat transfer is not entirely satisfactory, thus justifying a comprehensive investigation of this problem. And, further, a general approach for predicting pressure drop and heat transfer of enhanced tubes is needed.

The objectives of this work were two-fold: first, to carry out an extensive and consistent experimental investigation of pressure drop and heat transfer for laminar, transitional, and turbulent flow with smooth and internally enhanced tubes using air, water, and ethylene glycol/water mixtures as the working fluids; and second, to validate the previously developed corresponding states method for a range of Prandtl number values. This paper is devoted to the first objective; while verification of the corresponding states method by using experimental results obtained for the 0.7 to 125 Prandtl number range is considered in Part II.

EXPERIMENTAL FACILITY AND TEST PROCEDURES

General Description of Apparatus

For the air studies, the experimental facility and test procedures were described in detail elsewhere (Esen *et al.*, 1994; Esen, 1992); hence, these details are not given in this paper. The closed-loop liquid test facility is shown schematically in Fig. 1. The main components include a storage tank, a variable-speed gear pump, a surge tank, three rotameters, the test section consisting of the entrance section and the heated section, and a Basco Series 500 single-pass shell-and-tube heat exchanger having an outside surface area of 0.5 m^2. The pressure in the surge tank is limited to 310 kPa by a cut-off switch connected to the motor-controller power supply.

General Description of Enhanced Tubes

Twenty-three enhanced tubes and a smooth tube were tested in this study; the geometric characteristics of the smooth tube and the enhanced surfaces are given in Table 1. In the first column of Table 1, S, GA, HC, W, and Y denote smooth, General Atomic, Hitachi Cable, Wieland-Werke AG, and IMI Yorkshire Alloy, respectively. The last four are the suppliers of the tubes used in this study. A close-up photograph of all tubes is presented in Esen *et al.*, 1994.

In this study, the characteristic dimension in the definition of the nondimensional pressure drop, flow-rate, and heat-transfer coefficient is the maximum internal tube diameter; the mean values determined in our laboratory are given in Table 1. For helix angle, the values for the Hitachi tubes (HC-4, HC-5, HC-6) are the manufacturer's data; values for the remaining tubes were calculated from the relation $\alpha = \pi D_i/pN_s$, where p is the axial pitch and N_s is the number of starts.

It is evident from Table 1 that the twenty-three enhanced tubes have a common feature, that is, the internal surface geometries are spirally shaped. For each of the

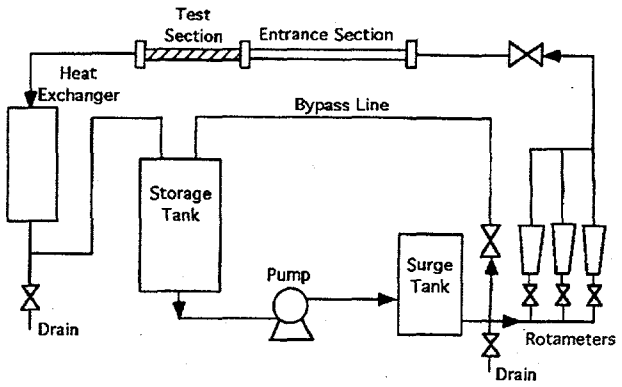

Fig. 1. Schematic diagram of closed-loop liquid test facility

spirally fluted tubes (GA-1 through GA-3, Y-22 and Y-23), the internal surface contour is similar to that on the outside surface. The HC-4 and the W-7 through W-13 tubes are basically spirally ribbed surfaces. Because the latter are also referred to by the manufacturer as spirally finned tubes, both terminologies are used interchangeably in this paper.

The two Hitachi tubes (H-5 and H-6) complement one another in that the surface protrusions are cross-cut to provide multistart three-dimensional spiral ribs. Details of the procedures used to generate these surface contours are given by Takahashi *et al.* (1985). For these tubes, the primary ribs form an angle α_1 with the tube axis, while the row of dents on the primary ribs form a different angle α_2 against the tube axis. When the ribs are oriented in the same rotational direction as the primary rib, α_2 is positive, and negative when the orientation of the dents is opposite that of the primary ribs. The height of the primary rib is e_1, while the depth of the dents is e_2. The axial pitch of the primary rib measured along the tube axis is p_1 and that of the dents is p_2.

The remaining eight tubes, (Y-14 to Y-21), were supplied by IMI Yorkshire Alloys and are referred to as spirally roped tubes by the supplier. They are characterized by indentations on the outside surfaces with ridges on the inner surfaces and are called spirally indented tubes in this paper.

Test Procedures

The basis for the design of the heated section was that of same heat transfer area. The exceptions were GA-3, Y-17, Y-19, and Y-21–Y-23, all of which were characterized by higher D_i values and larger heat transfer areas. Expressed in terms of D_i, the length of the heated section, L_h, ranged from about 9.5 D_i to 39 D_i, the lower values corresponding to the larger-diameter tubes. In other words, L_h varied slightly from tube to tube over the range of values from 475 mm for Y-19 to 313 mm for Y-16; the heated length for the smooth tube was 458 mm. Details on the experimental design are provided in the original report (Obot, 1995).

For each tube, the pressure-drop data were obtained in the presence of, as well as in the absence of, heat transfer

Table 1. Geometric Characteristics of Tubes

Tube	D_i (mm)	t (mm)	e (mm)	N_s	l (mm)	p (mm)	α (degrees)	e/D_i	p/e	Material	Roughness Description
S-0	13.39	1.2								copper	smooth
GA-1	21.45	0.7	0.95	20	82.0	4.1	39.4	0.044	4.3	stainless steel	spirally fluted
GA-2	23.96	0.98	1.33	25	141	5.6	28.1	0.056	4.2	stainless steel	spirally fluted
GA-3	28.49	1.89	1.58	31	160	5.2	29.2	0.055	3.3	aluminum	spirally fluted
HC-4	13.87	1.0	0.3	10	82.0	8.2	28.0	0.022	27.3	copper	spirally ribbed
HC-5	17.78	0.64	0.5	25	142.5	5.7	21.5	0.028	11.4	copper	3-D spirally
			(0.3)	(25)	(93.0)	(3.7)	(-31.0)	(0.017)	(12.3)		ribbed
HC-6	17.61	0.72	0.26	25	140.0	5.6	21.5	0.015	21.5	copper	3-D spirally
			(0.14)	(25)	(92.1)	(3.7)	(-31.0)	(0.008)	(26.4)		ribbed
W-7	14.10	1.07	0.42	1	2.2	2.2	87.2	0.030	5.2	copper	spirally ribbed
W-8	14.40	1.12	0.10	1	1.0	1.0	88.7	0.007	10.0	copper	spirally ribbed
W-9	15.90	1.52	0.5	41	102.5	2.5	26.0	0.032	5.0	copper	spirally ribbed
W-10	14.95	1.48	0.55	25	110.0	4.4	23.1	0.037	8.0	copper	spirally ribbed
W-11	14.45	1.49	0.45	20	76.0	3.8	30.9	0.031	8.5	copper	spirally ribbed
W-12	14.56	1.59	0.50	10	40.0	4.0	48.8	0.034	8.0	copper	spirally ribbed
W-13	14.45	1.50	0.51	25	120.0	4.8	20.7	0.035	9.4	copper	spirally ribbed
Y-14	12.68	1.08	0.38	3	15.0	5.0	69.4	0.030	13.2	copper	spirally indented
Y-15	19.16	1.24	1.27	3	30.0	10.0	63.5	0.066	7.9	copper	spirally indented
Y-16	19.53	1.23	0.51	3	30.0	10.0	63.9	0.026	19.6	copper	spirally indented
Y-17	24.22	1.67	0.31	3	15.0	5.0	78.8	0.013	16.1	copper	spirally indented
Y-18	18.81	1.66	0.36	3	7.8	2.6	82.5	0.019	7.2	copper	spirally indented
Y-19	22.88	1.04	1.5	6	198	33	20.0	0.066	22	K10	spirally indented
Y-20	16.05	1.36	1.0	3	30.0	10.0	59.2	0.062	10.0	copper	spirally indented
Y-21	23.45	0.93	0.52	1	6.0	6.0	85.3	0.022	11.5	K10	spirally indented
				(6)							doubly enhanced
Y-22	48.65	0.87	2.0	43	273.1	6.35	29.2	0.041	3.2	YAB	spirally fluted
Y-23	47.67	1.29	2.96	25	277.5	11.1	28.4	0.062	3.8	copper	spirally fluted

thus affording an extensive documentation of the effect of heat transfer on pressure drop. The frictional pressure coefficients (or values of the Fanning friction factor) were computed from the relation

$$f = \Delta p \rho_w A_x^2 D_i / 2m^2 L_p, \quad (1)$$

where ρ_w is the test fluid density evaluated at the average surface temperature.

For heat transfer, each test section was heated with nichrome wire, located in small grooves machined on the outside surface of a tube, by DC power source. The temperatures close to the inner surface of a test section were measured with 24 chromel-alumel thermocouples (36 gauge) located at six axial stations, with four thermocouples equally spaced circumferentially at each station.

With regard to the test procedures, the first involved establishing steady-state conditions for a desired flow rate in the absence of heating and then recording of all temperature and pressure readings. Next, power was supplied to the test section. The power supply controls were fine-tuned periodically to obtain the desired mean surface temperature and the deviation about this mean value; both were held fixed with increasing flow rate for each tube. Steady-state conditions with heating were reached when the fluid and surface temperatures remained unchanged for about 30 min. Then, all temperature and pressure readings were recorded.

Results for the average heat transfer coefficient, expressed in nondimensional form as the values of average Nusselt number (Nu), were computed from

$$Nu = (D_i Q_c)/(k_b A_h)\,(T_w - T_b), \quad (2)$$

where $T_b = (T_o + T_i)/2$ and the convective heat transfer rates were computed from

$$Q_c = Q_T - Q_L \quad (3)$$

and

$$Q_c = m\, C_p (T_o - T_i). \quad (4)$$

In Eq. (3), Q_T and Q_L represent the total electrical power input with and without fluid flow, respectively. The losses, Q_L, determined experimentally in the absence of the fluid flow, corresponded to the total electrical power input required to maintain the test section at the same average surface temperature as in tests with fluid flow.

For air (Pr = 0.7), the Q_c values were calculated from Eq. (3) for all test trials. The differences in the calculated values between Eqs. (3) and (4) were within ±10% (Esen, 1992). For water, Eq. (4) was the basis for all Q_c values used in the computation of the results in Das (1993). However, the laminar flow data of that study were reanalyzed with Eq. (3), in line with the data-reduction procedure for the glycol/water mixtures. The determination of laminar flow Q_c values from the total electrical power input is more accurate than the use of Eq. (4) due to cross-sectional variations in the fluid temperature at the exit of the test section. This method is recommended. For liquids in turbulent flow, Q_c values were computed by Eq. (4); there were almost no variations in the fluid temperature at the exit of the test section.

The Reynolds number (Re) ranges covered in the study were 200-55,000, 300-51,000, 300-12,000, 200-7,100 and 200-4,000 for Pr = 0.7, 6.8, 24.8, 39.1 and 125.3, respectively. For Pr = 39.1 and 125.3, tests were performed with only the smooth tube because laminar flow prevailed over a wide flow-rate range and it was expected that the results would afford a definite statement on the dependence of the nondimensional heat transfer coefficient on the Reynolds number. Equipment limitations precluded testing of the enhanced tubes at higher Reynolds numbers with Pr = 24.8.

For air (Pr = 0.7) and water (Pr = 6.8), the fluid properties used in the data reduction were based on the tabulations provided in Holman (1990). For pure glycol and glycol/water mixtures, the fluid properties were determined from the tables and graphical illustrations in the booklet provided by the Industrial Chemicals Division of Union Carbide, the supplier of the ethylene glycol. In addition, the viscosity of the glycol or glycol/water mixtures was checked periodically during the course of the experiments with a Brookfield LV Viscometer. The liquid density was also determined by weighing known volumes.

RESULTS AND DISCUSSION

Before the presentation and discussion of results, several points should be made. First, a complete tabulation of the results for friction factor, Nusselt number, and Reynolds number was given in the report that forms the basis for this paper (Obot, 1995). Second, heat-transfer tests were not carried out with the GA-1 and GA-2 tubes. Also, the two large-diameter tubes (Y-22 and Y-23) were not tested with glycol/water mixture because the attainable Reynolds numbers would be too low. Third, due to space limitations, graphical illustrations for some of the enhanced tubes are not included in this paper; these were presented in the original report (Obot, 1995).

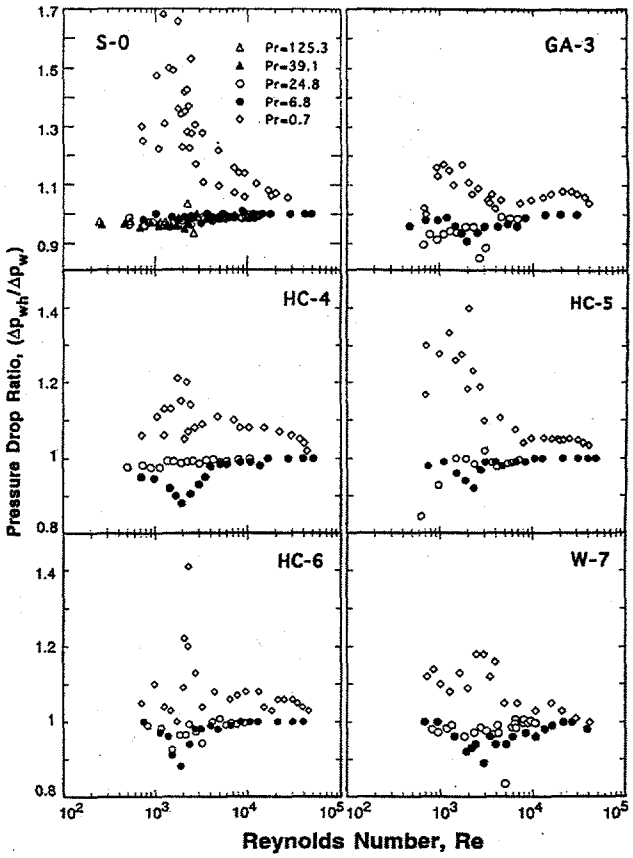

Fig. 2. Pressure drop ratio versus Re for tubes S-0 to W-7

Effect of Heat Transfer on Pressure Drop

In previous publications (Esen, 1992; Obot *et al.*, 1994), it was established that useful information on the effect of heat transfer on pressure-drop can be obtained by using pressure-drop ratios. Accordingly, typical plots of pressure-drop ratio ($\Delta p_{wh}/\Delta p_w$) versus Reynolds number (Re) are presented compactly in Fig. 2. Similar trends were obtained with the other tubes (Obot, 1995). In Fig. 2, Δp_{wh} is the steady-state pressure drop with heat transfer at the average surface temperature of the experiment, while Δp_w is the corresponding value recorded in the absence of heat transfer; that is, just before the onset of heating of the test section.

For each tube, the results show that the greatest effect of fluid heating on pressure drop occurs in the transition region. For liquids (Pr = 6.8 and 24.8), the recorded pressure-drop with heating is generally lower than that recorded without heating in the transition regime for a given Reynolds number; however, the trend is exactly the opposite for air (Pr = 0.7). The viscosity increases and decreases with temperature for air and liquids, respectively, hence the reversal in the ($\Delta p_{wh}/\Delta p_w$) versus Re trends. For most tubes, the value is close to 1 in the fully turbulent regime.

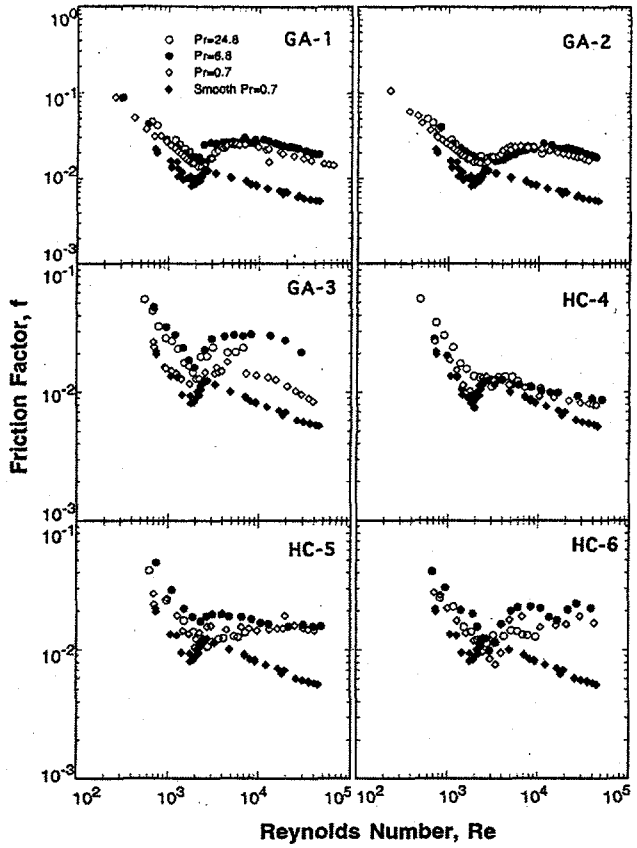

Fig. 3. Friction factor versus *Re* for tubes GA-1 to HC-6

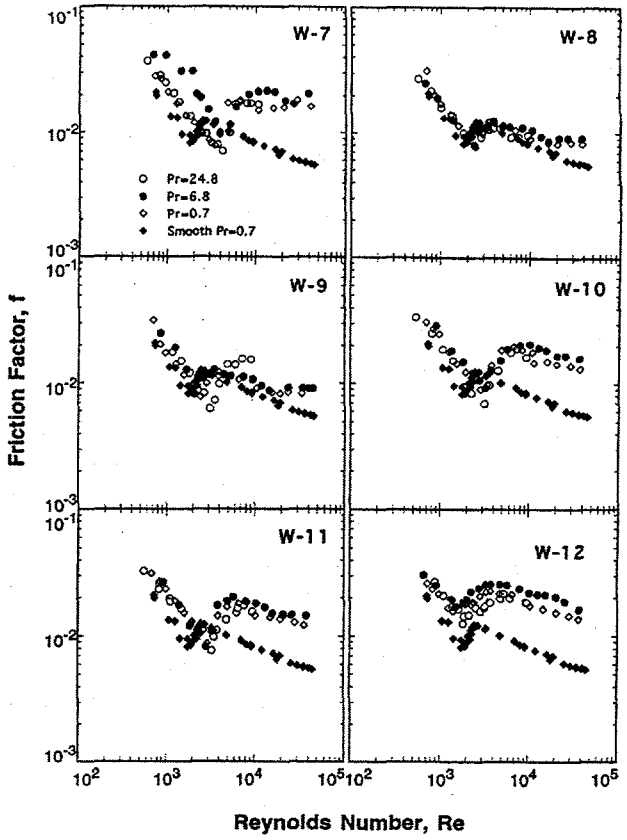

Fig. 4. Friction factor versus *Re* for tubes W-7 to W-12

The indication is that a plot of the pressure drop ratio against Reynolds number can be used to determine the Reynolds number at the onset of transition to turbulent flow. For liquids, the Reynolds number at transition can be determined with remarkable consistency as the location of the minimum values of $(\Delta p_{wh}/\Delta p_w)$. For air, the transition Reynolds number almost corresponds to the location of the peak value of $(\Delta p_{wh}/\Delta p_w)$. In passing, it is noted that the transition Reynolds numbers reported subsequently were determined from the friction factor and Nusselt number versus *Re* curves and not from those for pressure-drop ratio.

It should be noted that the pressure-drop ratio is dependent on the magnitude of the total electrical power input or on the average surface temperature. For liquids, the pressure-drop ratio decreases with increasing average surface temperature (Das, 1993). This contrasts sharply with the trend obtained with air (Pr = 0.7), the results of which indicated that the higher the average surface temperature, the higher the value of the pressure-drop ratio for a given Reynolds number (Esen, 1992).

Enhanced-Tube Friction Factor Results

The pressure-drop data reduced as values of the Fanning friction factor (f) are given compactly in Figs. 3-6. The results for each enhanced tube are compared with the Pr = 0.71 smooth-tube results. It is of interest to note that the smooth-tube friction factors are practically the same for all Prandtl numbers (Obot *et al.*, 1997). The results obtained with heating are given for each tube and these are also used in all subsequent illustrations, unless stated otherwise. There are two exceptions: GA-1 and GA-2 tubes were not tested for heat transfer. Due to space limitation, the alternative representations of the friction factor/ Reynolds number data as plots of the friction factor ratio, f_e/f_s, versus *Re* are given on Fig. 7 for W-7 through W-12.

In laminar flow, the general behavior of the results with increasing *Re is* the same for all tubes; f *is* inversely proportional to *Re* or the product f *x Re* (= C_f) *is* constant. The departure from the smooth-tube data depends on the geometric characteristics of the enhanced tube and is most pronounced for tubes of the spirally fluted type (GA-1 through GA-3, Y-22 and Y-23).

The results indicate rather complex effects of the enhanced-tube geometric details and Prandtl number on the transition process. For a number of tubes, the transition Reynolds numbers (Table 2) determined from plots of f *x Re* (= C_f) versus *Re* are significantly greater than the smooth-tube values. As a result, crossings of the enhanced and smooth-tube f versus *Re* curves are observed within the transition region. The friction factor at transition also varies with the tube geometry and Prandtl number (Table 2), further complicating definite statements on the effects of geometric parameters (e/D_i, p/e and α) and Prandtl number on the transition friction factor or the transition Reynolds number.

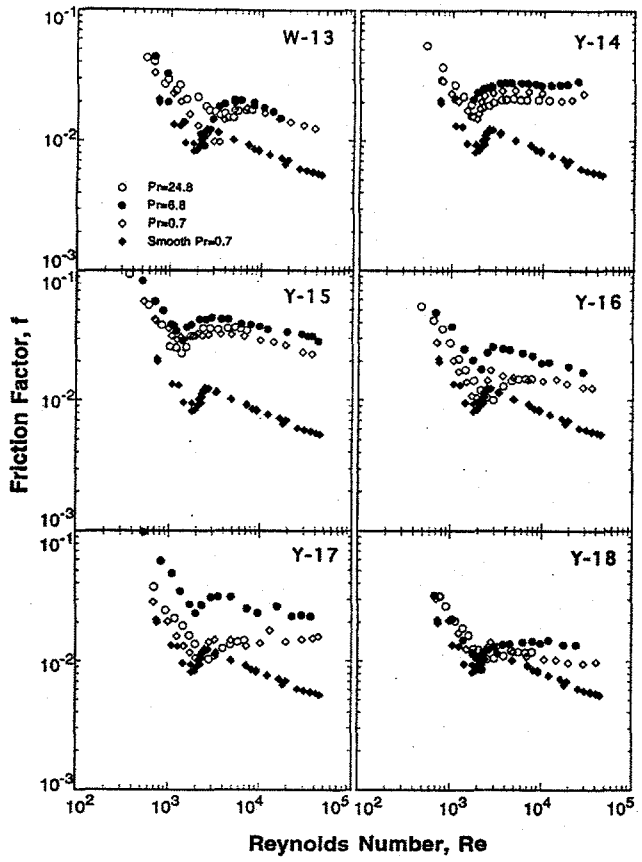

Fig. 5. Friction factor versus *Re* for tubes W-13 to Y-18

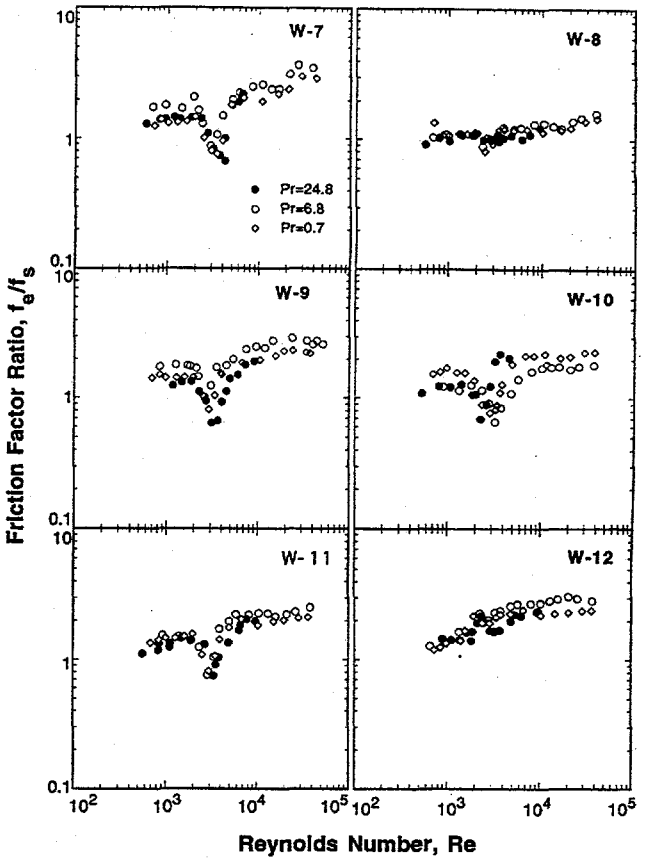

Fig. 6. Friction factor versus *Re* for tubes W-7 to W-12

The complications introduced by variations in the transition parameters (f_c and Re_c) are also reflected in the contrasting trends for the f_e/f_s versus *Re* curves (Fig. 7). For instance, the friction factor ratios for four of the seven W-tubes (W-7, 9, 10, and 11) lie well below unity; the transition Reynolds numbers for these tubes are much higher than the smooth-tube values (Table 2). By contrast, virtually all of the remaining tubes gave f_e/f_s values that were on the order of 1 or higher.

In turbulent flow, values of friction factor for any particular enhanced tube are generally greater than the smooth-tube values. Of the twenty-three enhanced tubes tested, only six (GA-1 through GA-3, Y-14, Y-15 and Y-20) are characterized by f_e/f_s values that are greater than 3 but under 5.5; $f_e/f_s \leq 3$ for the other tubes. Table 2 shows that these six tubes give transition Reynolds numbers that are generally lower than the smooth-tube values. So, the unique behavior of these six tubes is most likely the result of the inseparable effects of α, e/D_i, and p/e and the early transition to turbulence.

A study of these figures reveals that the influence of Prandtl number depends on the enhanced-tube geometric characteristics. For some of the tubes, the friction factor is essentially independent of the Prandtl number, paralleling the smooth-tube behavior (Obot *et al.*, 1997). The variations with *Pr* are confined only to the laminar, transitional, or turbulent flow for some of the tubes. For four tubes (GA-3, Y-16, Y-17, and Y-21), the differences between the three sets of data are significant, and these are observed over the entire *Re* range covered in the study.

It is evident from Table 1 that the upper limit to the range of e/D_i tested is 0.066 and, for this case, $p/e = 2.2$ (Y-19); this value of e/D_i can be considered to be on the high side. Despite this, the friction factors for this tube are no greater than twice those for the smooth tube. This contrasts sharply with the friction factor trends for surfaces having transverse disruptions. For instance, the f_e/f_s values at comparable *Re* for the transverse inserts of Koch (1960) with $e/D_i = 0.045$ and 0.075 ($p/e = 9.8$ in each case) are about 17.5 and 20, respectively. These values, even that for the lower e/D_i of 0.045, are considerably greater than those for the spiral disruptions. Differences of these magnitude in the pressure-drop characteristics between the two types of surface disruptions cannot be explained in terms of the difference in p/e, because the f_e/f_s values for Y-20 ($e/D_i = 0.062$ and $p/e = 10$) are both much lower than those deduced from Koch's data for transverse ribs of $e/D_i = 0.045$.

Enhanced-Tube Heat-Transfer Results

The convective heat-transfer rates reduced as values of the average Nusselt number (*Nu*) are presented on Figs. 7-10. Consistent with the treatment of friction factor, the alternative representations as plots of the Nusselt number

Table 2. Critical Data at the Onset of Transition to Turbulent Flow

Tube	Re_c			$f_c \times 10^3$			Nu_c		
	Pr=0.7	Pr=6.8	Pr=24.8	Pr=0.7	Pr=6.8	Pr=24.8	Pr=0.7	Pr=6.8	Pr=24.8
S-0	2100	2040	1900	9.3	8.2	8.0	6.1	17.3	22.8
GA-1	1880	1520	1660	14.4	18.8	19.1	-	-	-
GA-2	1850	1870	1670	15.4	16.4	17.8	-	-	-
GA-3	1790	1980	1870	14.2	15.4	13.3	9.2	21.6	34.1
HC-4	1970	1940	1640	8.9	8.4	12.5	6.4	17.1	20.9
HC-5	2000	1950	2390	10.9	15.5	10.9	7.0	20.5	29.7
HC-6	2020	1790	2160	9.1	10.1	10.7	7.1	16.9	22.6
W-7	2970	2256	3120	7.6	11.9	7.7	8.6	21.5	28.9
W-8	2440	2290	2350	7.1	9.1	7.6	7.4	18.2	26.8
W-9	2870	2600	2670	8.2	10.0	7.8	9.0	21.5	29.5
W-10	2620	2220	2270	8.8	10.7	8.6	7.7	20.7	27.2
W-11	2970	2290	2640	8.1	10.1	8.1	9.2	20.6	27.6
W-12	1500	1550	1840	13.3	15.6	13.3	5.0	16.5	21.8
W-13	2730	2300	1460	9.4	10.9	18.8	8.3	22.2	22.7
Y-14	1750	1420	1580	13.4	16.3	15.9	6.6	17.7	18.0
Y-15	1230	1090	1180	26.4	34.0	23.6	7.6	18.3	22.9
Y-16	2070	2030	2100	9.9	16.4	10.7	8.4	22.0	25.5
Y-17	1870	2040	2330	11.0	10.9	19.0	7.5	21.0	28.2
Y-18	1980	1870	1820	10.5	10.6	13.3	7.9	20.5	23.3
Y-19	2200	1980	1680	12.7	19.2	12.9	10.4	23.1	23.2
Y-20	830	1000	1070	31.7	29.4	27.5	5.0	15.1	17.4
Y-21	2170	1930	2440	9.7	13.1	21.0	10.2	29.8	31.1
Y-22	2770	3910	-	14.9	15.9	-	15.7	36.0	-
Y-23	2370	3040	-	16.6	13.5	-	12.8	33.2	-

ratio Nu_e/Nu_s versus Re are given in Fig. 10 for W-9 through Y-14.

Figures 7-9 show that Nu increases steadily in laminar flow for all tubes; each curve rises after the point of transition, in line with the friction factor behavior, and then changes direction at the onset of fully-turbulent flow. Figure 10 shows that Nu_e/Nu_s *is* essentially independent of Re in laminar flow, an indication that $Nu \propto Re^{1/2}$ for all enhanced tubes, as documented in Obot *et al.* (1997) for the smooth-tube. In laminar flow, the ratio Nu_e/Nu_s varies from slightly above unity to about 2.5, depending on the geometric details of the enhanced tube and the Prandtl number. Whereas most of tubes gave Nu_e/Nu_s values that were about the same for all Pr, the Nusselt number ratios obtained for Pr = 24.8 with the spirally indented tubes as a group (Y-14 through Y-21) were consistently the lowest set.

In the transition region, the trend for the most part is one of a drop in Nu_e/Nu_s value, beginning at the onset of transition to turbulent flow. As noted already in connection with the discussion of the results for friction factor ratio, this is a reflection of the crossing of the Nu versus Re curves because the transition Reynolds numbers for the enhanced tubes are much higher than the smooth-tube value (Table 2). The transition Nusselt number values determined as the limiting points with increasing Re in laminar flow on plots of $C_h = Nu/Re^{1/2}$ versus Re are presented in Table 2.

Figures 7-9 show that $Nu \propto Re^n$ in turbulent flow. For a specified Re range, the empirically determined value for n depends on the enhanced-tube geometric details and Pr. The dependence of the Reynolds number exponent on the type of surface disruptions is well documented in the literature (see, for example, Carnavos, 1980). In that study, the observation was that spirally finned tubes deviated the most from the 0.8 exponent on Re.

Given the rather contrasting trends of the friction factor versus Reynolds number curves and the effect of the transition process, some variation in the empirically determined Reynolds number exponent must be expected. Because observations based solely on the conventional Nu versus Re plots provide only a partial picture of the friction and heat transfer process, there is the need for a more general treatment in terms of Nu, f, and Re. Such a treatment is considered subsequently in Part II.

In turbulent flow, the results in Fig. 10 indicate various levels of enhancement depending on the geometric characteristics of the enhanced tube and to a lesser extent on the Prandtl number. With the exception of several tubes of the Y-series, there is no strong indication that the enhanced-tube heat-transfer results are sensitive to variations in the Prandtl number for liquids. It is of interest to note that Carnavos (1980) reached a similar conclusion for forged-finned tubes based on tests with water and glycol/water mixtures.

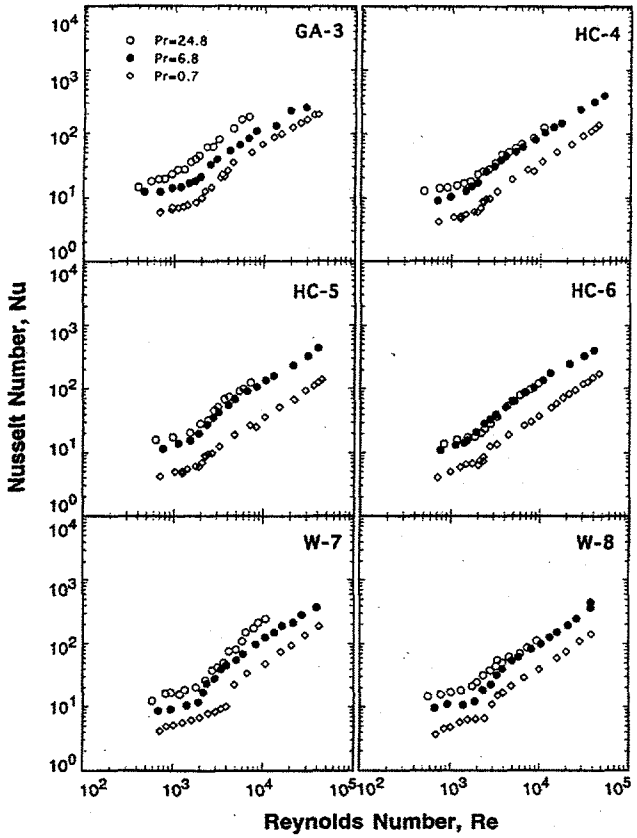

Fig. 7. Nusselt number versus *Re* for tubes GA-3 to W-8

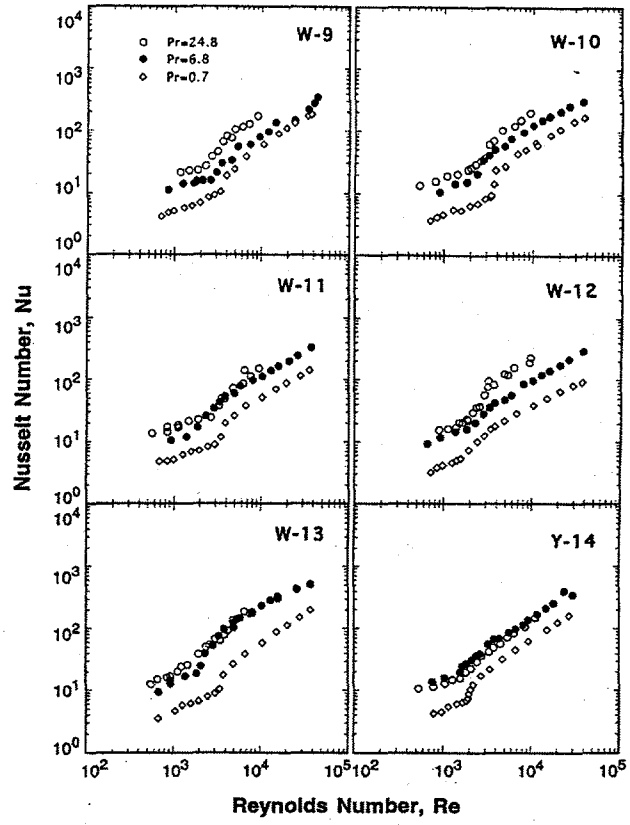

Fig. 8. Nusselt number versus *Re* for tubes W-9 to Y-14

A comparison of the f_e/f_s versus *Re* curves (Fig. 6) with the corresponding Nusselt number ratios of Fig. 10 reveals complete similarity in behavior between the two sets of results for any particular tube. For instance, the existence of a maximum or minimum in the f_e/f_s versus *Re* curve is also reflected in a maximum or minimum in the Nu_e/Nu_s versus *Re* plot. Also, when f_e/f_s increases with increasing *Re*, Fig. 10 shows that the same trend is exhibited by Nu_e/Nu_s. Although there are quantitative differences between the magnitude of f_e/f_s and Nu_e/Nu_s, the similarity in the general features of the curves begins in laminar flow and continues in the transitional and turbulent flow regimes.

Data Correlation

In principle, a generalized correlation for Nusselt number, *Nu*, can be presented in terms of the friction factor (*f*), Prandtl number (*Pr*), helix angle (α), relative height (e/D_i), and relative pitch (p/e). A thorough analysis of the results revealed that, expressed in terms of *f* and *Pr*, the correlation for laminar flow Nusselt number is independent of the geometric details of the enhanced tube (α, e/D_i and p/e). Accordingly, the results for smooth and enhanced tube are closely approximated by the relation

$$\overline{C_h}/C_f = Nu/(Re^{3/2} f Pr^{0.4}) = 0.008. \qquad (5)$$

The correlation predicts about 90% of the data points with errors that are mostly under 30%. There are indications that Eq. (5) is of general validity; no corrections are needed to account for the effect of transition to turbulence. A further elaboration on these observations is considered in Part II of this paper.

On a log-log plot of $\overline{C_h}/C_f$ versus *Re*, the data follow two distinct trends: the horizontal laminar flow segment, Eq. (5), and the decreasing trend with increasing Re for both the transition and turbulent flow regimes. For the latter, it is established that $Nu/(f\,Pr^{0.4}) \propto Re^n$, where $n = 1.05$. Unlike laminar flow, a single correlation of the *Nu* results in terms of *f*, *Pr*, and *Re* could not be established due to the residual effects of α, e/D_i and p/e that manifest themselves through variations in the transition parameters. The fact that $\overline{C_h}/C_f$ is constant in laminar flow for smooth and enhanced tubes, with significant spread of the data in transitional and turbulent flow, suggests a definite connection between the transition process and the attainable friction and heat transfer.

CONCLUSIONS

The results show that the effect of heat transfer on pressure drop is greatest in the transitional flow region, with moderate effect in laminar and turbulent flow. The effect of

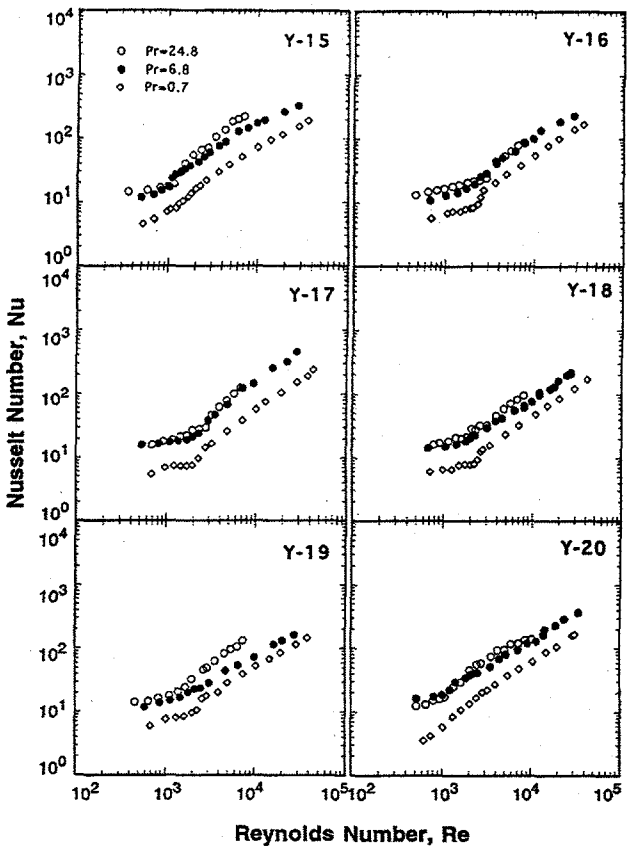

Fig. 9. Nusselt number versus *Re* for tubes Y-15 to Y-20

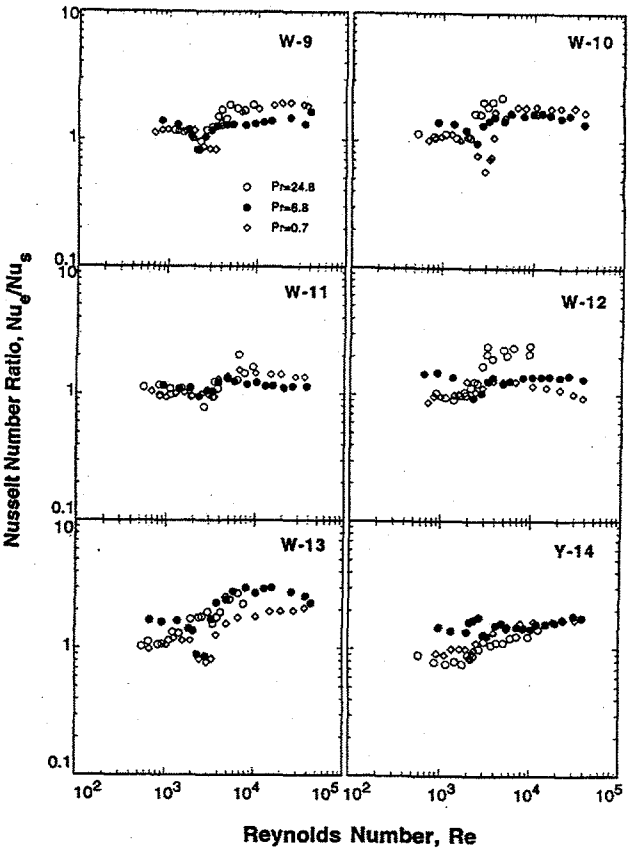

Fig. 10. Nusselt number versus *Re* for tubes W-9 to Y-14

wall cooling or fluid heating with liquids is exactly the opposite of that with air; a typical ($\Delta p_{wh}/\Delta p_w$) versus *Re* curve exhibits a well-defined minimum at the onset of transition to turbulence with liquids and a maximum with air.

The friction factor results indicate that, unlike transverse ribs or inserts, spirally shaped disruptions result in very moderate increases in pressure drop. The friction factors are usually no more than three times the smooth-tube values. The effect of Prandtl number on friction factor depends on the tube geometry and the flow type. For some tubes, the friction factors are practically the same for $0.7 \leq Pr \leq 25$, with differences in laminar, transitional, or turbulent flow for some of the tubes.

In laminar flow, $Nu \propto Re^{1/2}$ for all the enhanced tubes with $0.7 \leq Pr \leq 25$, paralleling the trend obtained with the smooth tube for $0.7 \leq Pr \leq 125.3$. Each *Nu* versus *Re* curve rises after the onset of transition to turbulent flow and then changes direction at the onset of fully turbulent flow. Consistent with the low-pressure-drop characteristics of these enhanced tubes, the increases in heat transfer coefficient are no more than 2.5 times the smooth-tube values for the range of *Pr* values covered in the study.

ACKNOWLEDGMENTS

This work, performed in the facilities at Clarkson University, was funded by the U.S. Department of Energy, Office of Conservation and Renewable Energy, Division of Advanced Industrial Concepts, E. P. HuangFu, Program Manager, Contract No. DE-FG02-89CE90029. Technical Support was provided by Dr. T. J. Marciniak, Manager, Experimental Systems Engineering, and by Dr. T. J. Rabas, Energy Systems Division, Argonne National Laboratory.

The authors thank Roger A. Green, Daniel Vakili, and Jeremie Dalton for their important contributions to this work. John Wescott made modifications to the test facility. The ethylene glycol was donated for the research by Union Carbide at the request of John Wescott.

Part of this work has been supported by the U.S. Department of Energy, Energy Efficiency and Renewable Energy, under Contract W-31-109-Eng-38.

REFERENCES

Carnavos, T. C., 1980, Heat Transfer Performance of Internally Finned Tubes in Turbulent Flow, *Heat Transfer Eng.*, Vol. 1, pp. 32-37.

Das, L., 1993, Pressure Drop and Heat Transfer for Water Flow Through Enhanced Passages, MS Thesis, Clarkson University.

Dipprey, D. F., and Sabersky, R. H., 1963, Heat and Momentum Transfer in Smooth and Rough Tubes at Various Prandtl Numbers, *Int. J. Heat Mass Transfer*, Vol. 6, pp. 329-353.

Esen, E. B., Obot, N. T., and Rabas, T. J., 1994, Enhancement: Part I. Heat Transfer and Pressure Drop Results for Air Flow Through Enhanced Passages with Spirally-Shaped Roughness, *J. Enhanced Heat Transfer*, Vol. 1, #2, pp. 145-156.

Esen, E. B., 1992, Pressure Drop and Heat Transfer for Air Flow Through Enhanced Passages, PhD Thesis, Clarkson University.

Gomelauri, V., 1964, Influence of Two-Dimensional Artificial Roughness on Convective Heat Transfer, *Int. J. Heat Mass Transfer*, Vol. 7, pp. 653-663.

Holman, J. P., *Heat Transfer*, 7th Ed., McGraw-Hill, New York.

Koch, R., 1960, Pressure Loss and Heat Transfer for Turbulent Flow, U.S. Atomic Energy Commission, AEC-tr-3875.

Marner, W. J., and Bergles, A. E., 1978, Augmentation of Tubeside Laminar Flow Heat Transfer by Means of Twisted-Tape, Static-Mixer Inserts, and Internally Finned Tubes, *Proc. 6th Int. Heat Transfer Conf.*, Vol. 2, pp. 583-588.

Nunner, W., 1956, Heat Transfer and Pressure Drop in Rough Tubes, Atomic Energy Research Establishment (U.K.), Lib/Trans. 786.

Obot, N. T., 1995, Smooth-and-Enhanced-Tube Heat Transfer and Pressure Drop for Air, Water and Glycol/Water Mixtures, Final Report DOE/CE/90029-9.

Obot, N. T., Das, L., Vakili, D. A., and Green, R. A., 1977, Effect of Prandtl Number on Smooth-Tube Heat Transfer and Pressure Drop, *Int. Comm. Heat Mass Transfer*, Vol. 24, #6, pp. 889-896.

Obot, N. T., Esen, E. B., and Rabas, T. J., 1994, Enhancement: Part 11. The Role of Transition to Turbulent Flow, *J. Enhanced Heat Transfer*, Vol. 1, #2, pp. 157-167.

Obot, N. T., Esen, E. B., and Rabas, T. J., 1990, The Role of Transition in Determining Friction and Heat Transfer in Smooth and Rough Passages, *Int. J. Heat Mass Transfer*, Vol. 33, pp. 2133-2143.

Panchal, C. B., and France, D. M., 1986, Performance Tests of the Spirally Fluted Tube Heat Exchanger for Industrial Cogeneration Applications, Argonne National Laboratory Report ANL/CNSV-59.

Rabas, T. J., 1989, Selection of the Energy-Efficient Enhancement Geometry For Single-Phase Turbulent Flow Inside Tubes, Heat Transfer Equipment Fundamentals, Design, Applications and Operating Problems, HTD-Vol. 108, R. K. Shah, ed., American Society of Mechanical Engineers, New York, pp. 193-204.

Ravigururajan, T. S., and Bergles, A. E., 1986, Study of Water-Side Enhancement for Ocean Thermal Conversion Heat Exchangers, HTL-44/ERI Project 1718, Iowa State University.

Reay, D. A., 1991, Heat Transfer Enhancement - A Review of Techniques and TheirPossible Impact on Energy Efficiency in the U.K., *Heat Recovery Systems ~ CHP*, Vol. 11, pp. 1-90.

Shome, B., and Jensen, M. K., 1996, Experimental Investigation of Laminar Flow and Heat Transfer in Internally Finned Tubes, *J. Enhanced Heat Transfer*, Vol. 4, pp. 53-70.

Smith, J. W., and Gowen, R. A., 1965, Heat Transfer Efficiency in Rough Pipes at Prandtl Number, *AIChE J.*, Vol. 11, pp. 941-43.

Takahashi, K., Nakayama, W., and Kuwahara, H., 1985, Enhancement of Forced Convective Heat Transfer in Tubes Having Three-Dimensional Spiral Ribs, *Trans. JSME*, Vol. 51-461, pp. 350-355.

Watkinson, A. P., Miletti, D. L., and Kubanek, G. R., 1974, Heat Transfer and Pressure Drop of Forge-Fin Tubes in Laminar Oil Flow, Noranda Research Center, Internal Report # 303.

Webb, R. L., 1987, Enhancement of Single-Phase Heat Transfer, in *Handbook of Single-Phase Convective Heat Transfer*, S. Kakac, R. K. Shah, and W. Aung, eds., John Wiley and Sons, New York.

Webb, R. L., Eckert, E. R. G., and Goldstein, R. J., 1971, Heat Transfer and Friction in Tubes with Repeated-Rib Roughness, *Int. J. Heat Mass Transfer*, Vol. 14, pp. 601-617.

Withers, J. G., 1980a, Tube-Side Heat Transfer and Pressure Drop for Tubes Having Helical Internal Ridging with Turbulent/Transitional Flow of Single-Phase Fluid. Part 1. Single-Helix Ridging, *Heat Transfer Eng.*, Vol. 2, # 1, pp. 48-58.

Withers, J. G., 1980b, Tube-Side Heat Transfer and Pressure Drop for Tubes Having Helical Internal Ridging with Turbulent/Transitional Flow of Single-Phase Fluid. Part 2. Multiple-Helix Ridging, *Heat Transfer Eng.*, Vol. 2, # 2, pp. 43-50.

Yampolsky, J. S., Libby, P. A., Launder, B. E., and LaRue, J. C., 1984, Fluid Mechanics and Heat Transfer Spiral Fluted Tubing, GA Technologies Report GA-A17833.

NOMENCLATURE

A_h	heat transfer area
A_x	cross-sectional flow area
C_f	friction parameter, $f x Re$
C_h	heat transfer parameter, $Nu/Re^{1/2}$
$\overline{C_h}$	heat transfer parameter, $Nu/Re^{1/2}\ Pr^{0.4}$
C_p	specific heat
D_i	maximum internal diameter of tube
e	roughness height
f	Fanning friction factor
h	average heat transfer coefficient
k_b	thermal conductivity at T_b
L_e	smooth entrance length
$L_{e,r}$	rough entrance length
L_h	length of heated section
L_p	distance between pressure taps
l^p	lead
m	mass flow rate
N_s	number of starts
Nu	Nusselt number

p	roughness pitch
Pr	Prandtl number
Δp	pressure drop
Δp_w	pressure drop without heat transfer
$\Delta p_{w,h}$	pressure drop with heat transfer
Q_c	convective heat transfer rate
Q_L	total electrical power without flow at T_w
Q_T	total electrical power with flow at T_w
Re	Reynolds number
T	temperature
T_b	bulk mean temperature, $(T_i + T_o)/2$
T_w	average surface temperature
t	wall thickness

Greek Symbols

α	helix angle
μ	fluid viscosity
ρ_w	fluid density evaluated at T_w

Additional Subscripts

e	enhanced tube
i	condition at inlet to test section
o	condition at test section exit
s	smooth tube